An Anderson impurity in conjugated polymers. I. A new localized state in the electronic gap for the impurity with U=0

1991 J. Phys.: Condens. Matter 3 4841

(http://iopscience.iop.org/0953-8984/3/26/007)

J. Phys.: Condens. Matter 3 (1991) 4841–4856. Printed in the UK

An Anderson impurity in conjugated polymers: I. A new localized state in the electronic gap for the impurity with $U = 0$

Kikuo Harigaya†
Department of Physics, Faculty of Science, University of Tokyo, Hongo 7-3-1, Bunkyo-ku, Tokyo 113, Japan

Received 16 November 1990, in final form 15 January 1991

Abstract. An Anderson impurity in conjugated polymers is formulated in order to investigate the effects of a dopant, a carbonyl (>C═O) defect or an atomic side group. The impurity effects with no Coulomb interaction ($U = 0$) are studied analytically in the Takayama–Lin-Liu–Maki (TLM) model and also in the Su–Schrieffer–Heeger (SSH) model. A new localized level is found in the electronic gap. It is located at the top of the valence band when the level of the impurity is deep and in the valence band. It is at the bottom of the conduction band if the energy of the impurity level is in the conduction band. Characteristic TLM results agree remarkably well with the corresponding SSH results when the solutions in the TLM model are energetically stable against change of electron number. This agreement does not depend on whether the chain is nearly dimerized or there is a soliton excitation. Consequences for possible experimental observation of the localized state due to the real defect are discussed.

1. Introduction

In a series of works [1–9], we have been investigating impurity effects in conjugated polymers. Two types of impurity models are considered. One is site type [1, 3, 7], which locally modulates the site energy of electrons at impurity sites. The other is bond type [1, 2], which affects the hopping integral of π electrons. These impurities give additional potentials to electrons in a chain. Electrons are scattered by the potentials so that electronic states in the Peierls gap are drastically altered. On the other hand, there might be cases where interactions between the impurity itself and polymer chains are important. These have not been considered in the above investigations.

In this paper, we make use of the Anderson impurity model [10] in order to describe cases where interactions between a polymer chain and an additional localized level are strong. Possible situations where the Anderson impurity model might be applied are: electron hopping process between a dopant atom and a polymer chain; a local carbonyl (>C═O) defect that is naturally present both in pristine polyacetylene and in polyacetylene exposed in air; and effects of an atomic side group that strongly accepts electrons from or donates them to the chain. We note that Mizes and Conwell [11] have recently proposed the use of the Anderson model (with no Coulomb interactions) to describe a carbonyl (>C═O) defect, too. The transmission coefficient of π electrons around the impurity has been analysed in association with the conduction.

† Present address: Fundamental Physics Section, Physical Science Division, Electrotechnical Laboratory, Umezono 1-1-4, Tsukuba 305, Japan.

0953-8984/91/264841 + 16 $03.50

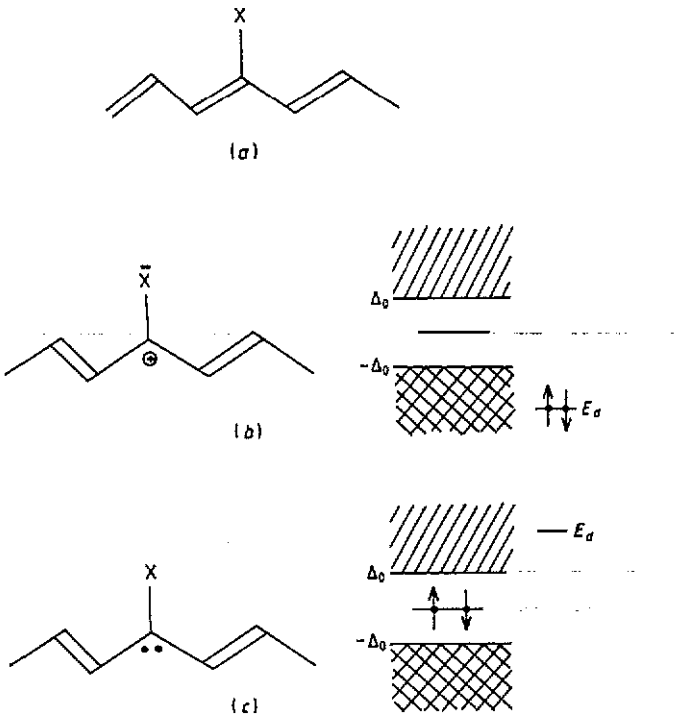

Figure 1. Schematic structures of an Anderson impurity in conjugated polymers. Electronic level structures are also shown. In (*a*), a pristine configuration with the nearly dimerized chain is shown. An Anderson impurity is denoted by the atom 'X'. In (*b*) and (*c*), the cases with a soliton are shown for deep and high impurity levels, respectively.

We depict our model system schematically in figure 1. We consider an imaginary side atom, namely 'X', adjacent to a carbon atom of a polymer chain. In the atom X, there is assumed to be one localized level. As the atom X and the chain strongly interact via the mixing interaction, electronic states of the polymer chain would drastically change around the atom X. There would be an effective site-type impurity [3, 7] at the atom X. As shown in previous papers [3, 7], electronic structures change due to the presence of the site-type impurity. Similar effects are expected to occur when there is an Anderson impurity. In this paper, we would like to investigate the variation of electronic states. We concentrate upon the system without Coulomb interaction at the atom X. Effects of the Coulomb force are to be investigated in the next paper.

Interactions between the atom X and the chain would be indeed quite interesting. When the atom X attracts electrons strongly, and thus a local level of the atom X is deep enough in the valence band, the pristine configuration in figure 1(*a*) would change into the configuration in figure 1(*b*). As the X atom would act as an effective site-type impurity, it would be energetically favourable to create a pinned soliton around the atom X. In figure 1(*b*), two electrons occupy the localized level, namely E_d, and π-electron states in the chain are filled with electrons, the number of which is reduced by unity from half-filled. A positively charged soliton is pinned at the site adjacent to the atom X. There would be an additional localized level at the top of the valence band due to the effective site-type impurity with positive strength. On the other hand, when the atom X donates electrons to the chain, the local level at the atom X would be at high

energy in the conduction band. The configuration in figure 1(*a*) would change into that of figure 1(*c*). The localized level at the atom X is unoccupied. The number of electrons of the chain increases by unity from half-filled. There is a negatively charged soliton pinned at the atom X. A new localized level would appear at the bottom of the conduction band due to the effective negative site-type potential. In this way, our system may show fertile changes of electronic structures, which depend on given parameters, namely electron number and the energy of the localized level at atom X.

In the present paper, the single-impurity problem is studied analytically in the Takayama–Lin-Liu–Maki (TLM) model [12] and also numerically in the Su–Schrieffer–Heeger (SSH) model [13]. A new localized level is found in the electronic gap. It is located at the top of the valence band when the level of the impurity is deep and in the valence band. It is at the bottom of the conduction band if the energy of the impurity level is in the conduction band. Characteristic TLM results agree remarkably well with the corresponding SSH results when the solutions in the TLM model are energetically stable against change of electron number. The consequences for possible experimental observation of the real defect state are discussed.

The paper is organized as follows. In section 2, the model is explained. Systems with even sites are investigated in section 3. Systems with odd sites are studied in section 4. Summary and discussion are given in section 5. In the appendix, the relation between the Anderson impurity and the site-type impurity is discussed.

2. Model

We first consider the following model:

$$H = H_{\mathrm{SSH}} + H_{\mathrm{A}}. \tag{2.1}$$

The first term is the SSH Hamiltonian [13]

$$H_{\mathrm{SSH}} = -\sum_{n,s}[t_0 - \alpha(u_{n+1} - u_n)](c^{\dagger}_{n+1,s}c_{n,s} + \mathrm{HC}) + \tfrac{1}{2}K\sum_{n}(u_{n+1} - u_n)^2 \tag{2.2}$$

where t_0 is the nearest-neighbour hopping integral of the undimerized chain, α is the electron–phonon coupling strength due to the modulation of the hopping integral, u_n is the displacement of the nth CH unit, $c_{n,s}$ is an annihilation operator of an electron at the nth site with spin s ($s = \uparrow$ or $\downarrow$) and K is the force constant between adjacent units. The second term is the Anderson impurity [10] localized at the lth site

$$H_{\mathrm{A}} = E_{\mathrm{d}}\sum_{s} d^{\dagger}_{s}d_{s} + V\sum_{s}(d^{\dagger}_{s}c_{l,s} + c^{\dagger}_{l,s}d_{s}) + Ud^{\dagger}_{\uparrow}d_{\uparrow}d^{\dagger}_{\downarrow}d_{\downarrow} \tag{2.3}$$

where d_s is an annihilation operator of a localized electron at the atom X, E_{d} is its atomic level, V is the mixing matrix element between the localized level and the π-electron orbital at the lth site of the polymer chain and U is the on-site Coulomb repulsion strength at the atom X. As we consider the case $U = 0$ in this paper, we neglect the last term of equation (2.3) hereafter. Effects of finite U are to be studied in the next paper [14].

The model (2.1) can be treated analytically in the continuum limit. Using the relations between the discrete and continuum operators, we obtain a continuum version of (2.1)

$$H' = H_{\mathrm{TLM}} + H'_{\mathrm{A}}. \tag{2.4}$$

The first term of (2.4) is the TLM model [12]

$$H_{\mathrm{TLM}} = \sum_{s}\int \mathrm{d}x\,\Psi^{\dagger}_{s}(x)\left(-\mathrm{i}v_{\mathrm{F}}\sigma_3\frac{\partial}{\partial x} + \Delta(x)\sigma_1\right)\Psi_s(x) + \frac{1}{2\pi v_{\mathrm{F}}\lambda}\int \mathrm{d}x\,\Delta^2(x) \tag{2.5}$$

where $\Psi_s(x)$ is a two-component field operator of π electrons with spin s, v_{F} is the Fermi

velocity, σ_i are the Pauli spin matrices, $\Delta(x)$ is the order parameter and $\lambda \equiv 2\alpha^2/\pi K t_0$ is the dimensionless electron–phonon coupling constant. The second term of (2.4) gives the impurity term

$$H'_A = E_d \sum_s d_s^\dagger d_s + a^{1/2} V \sum_s [d_s^\dagger \chi_l^\dagger \Psi_s(x_l) + \Psi_s^\dagger(x_l)\chi_l d_s] \tag{2.6}$$

where

$$\chi_l = \begin{pmatrix} \exp[-(\pi/2)li] \\ \exp[(\pi/2)(l+1)i] \end{pmatrix} \tag{2.7}$$

and $x_l = la$, a being the lattice constant of the undimerized system in the SSH model.

3. Systems with even sites

The system with even sites is perfectly dimerized when there is no impurity and electron states are half-filled. It contains a polaron when one electron is added to or removed from the system. In this section, we consider how electronic structure changes in the presence of an Anderson impurity at the lth site.

3.1. TLM model

In this subsection, analytic calculation is presented for the model (2.4) with the uniform dimerization $\Delta(x) = \Delta_0$.

We define the d-electron's Green function as

$$G_d(\tau) = -\langle T\tau\, d_s(\tau) d_s^\dagger(0)\rangle \tag{3.1}$$

where $d_s(\tau) = \exp(\tilde{H}\tau) d_s \exp(-\tilde{H}\tau)$ and $\tilde{H} = H' = \mu N_e$, μ being the chemical potential and N_e the electron number. Similarly, the π-electron Green function is defined by

$$G_c(k, p, \tau) = -\langle T\tau\, \Psi_s(k, \tau)\Psi_s^\dagger(p, 0)\rangle \tag{3.2}$$

where $\Psi_s(k, \tau) = \exp(\tilde{H}\tau)\Psi_s(k)\exp(-\tilde{H}\tau)$ and

$$\Psi_s(k) = \frac{1}{L^{1/2}} \int dx\, e^{-ikx}\Psi_s(x)$$

L being the system size.

Fourier transforms of Green functions,

$$G_d(i\varepsilon_n) = \int_0^{1/T} d\tau\, e^{i\varepsilon_n \tau} G_d(\tau)$$

and

$$G_c(k, p, i\varepsilon_n) = \int_0^{1/T} d\tau\, e^{i\varepsilon_n \tau} G_c(k, p, \tau)$$

are calculated from equations of motions to be

$$G_d(i\varepsilon_n) = \left(i\varepsilon_n + \mu - E_d - \frac{aV^2}{2\pi} \int dk\, \mathrm{Tr}[G_c^{(0)}(k, i\varepsilon_n)]\right)^{-1} \tag{3.3}$$

and

$$G_c(k, p, i\varepsilon_n) = G_c^{(0)}(k, i\varepsilon_n)\delta_{k,p} + V^2 G_c^{(0)}(i\varepsilon_n, k) G_d(i\varepsilon_n) G_c^{(0)}(i\varepsilon_n, p) \tag{3.4}$$

where

$$G_c^{(0)}(k, i\varepsilon_n) = (i\varepsilon_n + \mu - v_F k\sigma_3 - \Delta_0\sigma_1)^{-1}. \tag{3.5}$$

Using the relation

$$\frac{1}{2\pi}\int dk\, G_c^{(0)}(k, i\varepsilon_n) = -\frac{i\varepsilon_n + \mu + \Delta_0\sigma_1}{2v_F[\Delta_0^2 - (i\varepsilon_n + \mu)^2]^{1/2}} \tag{3.6}$$

we obtain

$$G_d(i\varepsilon_n) = \left(i\varepsilon_n + \mu - E_d + \frac{V^2}{2t_0}\frac{i\varepsilon_n + \mu}{[\Delta_0^2 - (i\varepsilon_n + \mu)^2]^{1/2}}\right)^{-1} \tag{3.7}$$

where $v_F = 2at_0$ is used. The condition of singularity of (3.7) yields

$$(\Delta_0^2 - \omega^2)^{1/2} = (V^2/2t_0)\omega/(E_d - \omega) \tag{3.8}$$

where $i\varepsilon_n + \mu$ is replaced by ω. This equation always has one solution in the region $|\omega| < \Delta_0$. Then, a new localized level appears when an Anderson impurity is located in the system. In the next subsection, the numerical solution of (3.8) will be represented by a thin curve in figure 4 and will be compared with solutions by the SSH model.

We briefly discuss properties of the solution. When the atomic d level is in the gap, i.e. $|E_d| \ll \Delta_0$, the approximate solution is

$$\omega \simeq \{\Delta_0/[\Delta_0 + (V^2/2t_0)]\}E_d. \tag{3.9}$$

Particularly, $\omega = 0$ when $E_d = 0$. This is due to the electron–hole symmetry.

When the atomic d level is widely separated from the energy gap, i.e. $|E_d| \gg \Delta_0$, we can neglect ω relative to E_d in the denominator of the right-hand side of (3.8). It is solved to get

$$\omega \simeq \Delta_0(\operatorname{sgn} E_d)/[1 + (V^2/2t_0E_d)^2]^{1/2}. \tag{3.10}$$

In [7], we have shown that the site-type impurity, $H_1 = J\sum_s c_{l,s}^\dagger c_{l,s}$, at the lth site gives rise to a localized level in the gap at energy

$$\omega = \Delta_0(-\operatorname{sgn} J)/[1 + (J/2t_0)^2]^{1/2}. \tag{3.11}$$

Equations (3.10) and (3.11) agree when we take $J = -V^2/E_d$. This is to be verified in the appendix, by performing a second-order perturbation with respect to the mixing term of (2.3). This agreement means physically that an Anderson impurity with negative E_d corresponds to an acceptor that gives a repulsive potential to π electrons. Similarly the model with positive E_d corresponds to a donor that gives rise to an attractive potential to π electrons.

3.2. SSH model

In order to compare with the results in section 3.1 and know the validity of setting $\Delta(x) = \Delta_0$, the model equation (2.1) with $U = 0$ is to be studied numerically. We consider the cases with $N_e = N, N + 1$ and $N + 2$, N being the system size of the SSH model. Periodic boundary conditions are imposed on electronic and lattice systems in order to remove end-point effects. We denote the κth π-electron wavefunction as $\varphi_\kappa(n)$ $(1 \leqslant n \leqslant N)$. It satisfies the boundary condition

$$\varphi_\kappa(n + N) = \varphi_\kappa(n). \tag{3.12}$$

The boundary condition for the lattice is

$$u_{n+N} = u_n. \tag{3.13}$$

The wavefunction is calculated from the eigenvalue problem

$$\varepsilon_\kappa\varphi_\kappa(n) = -(t_0 - \alpha y_{n-1})\varphi_\kappa(n-1) - (t_0 - \alpha y_n)\varphi_\kappa(n+1) + V\delta_{n,l}\varphi_\kappa(d) \tag{3.14}$$

and

$$\varepsilon_\kappa \varphi_\kappa(d) = E_d \varphi_\kappa(d) + V\varphi_\kappa(l) \tag{3.15}$$

where ε_κ is the eigenvalue, $y_n = u_{n+1} - u_n$ and $\varphi_\kappa(d)$ is the amplitude at the d site. The self-consistency condition for the lattice is

$$y_n = -\frac{2\alpha}{K}\sum_{\kappa,s}{}' \varphi_\kappa(n+1)\varphi_\kappa(n) + \frac{2\alpha}{KN}\sum_m \sum_{\kappa,s}{}' \varphi_\kappa(m+1)\varphi_\kappa(m) \tag{3.16}$$

where the prime indicates the sum over occupied states and the second term is due to the periodic boundary condition (3.13). The sum over m in the second term is taken over N sites of the polymer chain. The d site is not included in the sum, because electron–phonon interaction is not assumed at the bond between the d site and the lth site of the chain. Equation (3.16) is the same as that in [8, 9].

Numerical solution is obtained in the following way:

(i) First, random numbers between $-y_0$ and y_0 ($y_0 = 0.1$ Å) are generated for the initial values of the bond variables $\{y_n^{(0)}\}$. Then, we start the iteration.

(ii) At the kth step of the iteration, the electronic part of the Hamiltonian is diagonalized by solving equations (3.14) and (3.15) for the set of the bond variables $\{y_n^{(k)}\}$.

(iii) Using the electronic wavefunctions $\{\varphi_\kappa(j)|j = 1, \ldots, N, d\}$ obtained above, we calculate the next set $\{y_n^{(n+1)}\}$ from the left-hand side of equation (3.16).

(iv) The iteration is repeated until the sum $\Sigma_n(y_n^{(k+1)} - y_n^{(k)})^2$ becomes sufficiently small. Then, the stationary solution is obtained.

(v) It is checked that there are not other types of stationary solutions by changing the initial set $\{y_n^{(0)}\}$.

Numerical results are reported for the parameters $\alpha = 4.1$ eV Å^{-1}, $K = 21$ eV Å^{-2} and $t_0 = 2.5$ eV with $N = 50$. These give $\lambda = 0.20$. When the results are compared with those of section 3.1, $\lambda = 0.183$ is used for the TLM model. These two values give the same order parameter Δ_0 ($= 0.65$ eV $= 0.26t_0$) for the perfectly dimerized system. We particularly take $V = 0.5t_0$ because of the limitation of available CPU time.

3.2.1. $N_e = N$. In this part, we report numerical results for systems where electron number N_e is the same as that of the chain size N. As the total number of lattice sites is $N + 1$ and there are $2(n + 1)$ electronic states, electron number decreases from half-filling by unity.

In figure 2, we show lattice and charge configurations for $E_d = 0.6t_0$. In figure 2(a), the smoothed bond variable, $\bar{y}_n \equiv (-1)^n(y_n - y_{n-1})/2$, is shown. In figure 2($b$), the smoothed charge density, $\bar{\rho}_n \equiv (\rho_{n-1} + 2\rho_n + \rho_{n+1})/4$, is presented. The impurity is located at $n = 25$. In figure 2(b), the electron number of the d level is also shown by the vertical line. The localized level is almost empty. So, the chain system is nearly half-filled. There is an effective site-type impurity of strength $-V^2/E_d = -0.417t_0$ at $n = 25$. Thus, there is a localized level below the bottom of the conduction band, which is depicted in figure 4. The lattice distortion around the impurity found in figure 2(a) is characteristic to a site-type impurity reported in a recent paper [8]. It deforms asymmetrically with respect to the impurity position. This asymmetry reflects the difference of the strong and weak bonds. The asymmetrical distortion of $\bar{\rho}_n$ also reflects this property.

In figure 3, we show $\bar{y}_n$ and $\bar{\rho}_n$ for $E_d = -0.6t_0$. The localized d level is almost doubly filled. So, the electron number of the chain system is decreased from half-filling by about two. In the impurity-free system, two positively charged solitons would be formed. They would be separate from each other. In the present system, a charged soliton is pinned

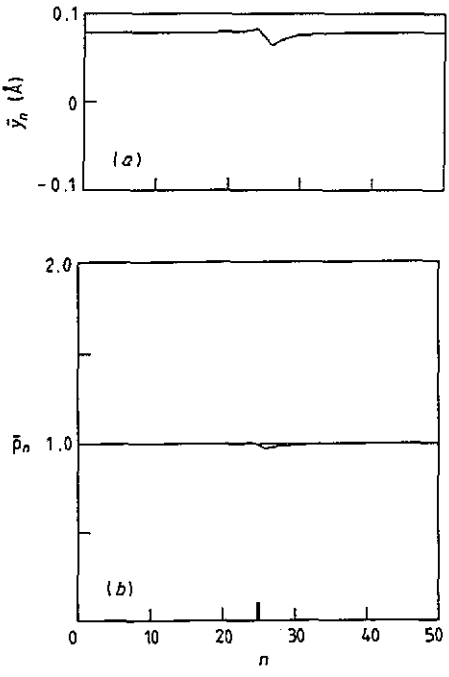

Figure 2. Dimerization pattern (*a*) and electron density (*b*) in the SSH model with an Anderson impurity at $n = 25$. In (*b*), electron number at the d level is also shown by the vertical bar. Parameters are $V = 0.5t_0$, $E_d = 0.6t_0$ and $N = N_e = 50$.

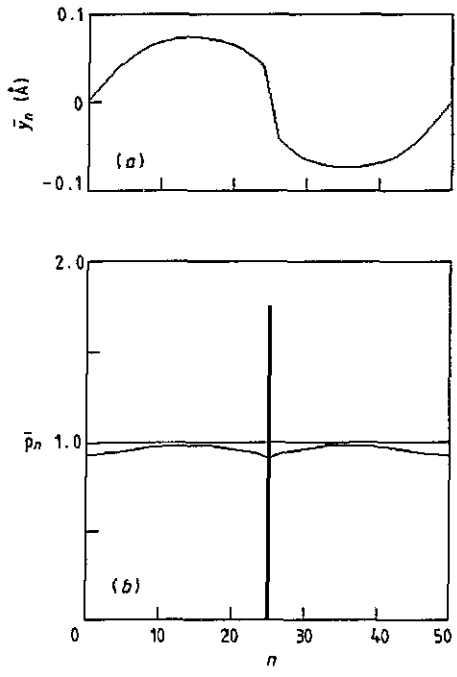

Figure 3. Dimerization pattern (*a*) and electron density (*b*) in the SSH model with an Anderson impurity at $n = 25$. In (*b*), electron number at the d level is also shown by the vertical bar. Parameters are $V = 0.5t_0$, $E_d = -0.6t_0$ and $N = N_e = 50$.

at the impurity. The lattice pattern and charge distribution around the impurity are similar to those of the site-type impurity problem reported in [8]. (The effective site-type strength is $V^2/E_d = 0.417t_0$.) Soliton width becomes narrower due to potential pinning. The free soliton at $n = 50$ has width similar to that in the impurity-free system.

We show changes of electronic levels around the energy gap as a function of E_d in figure 4. The d level is changed within $-1.0t_0 \leqslant E_d \leqslant 1.0t_0$. The broken curve indicates the Fermi level. The position is the average of energies of the highest occupied and the lowest unoccupied states. Levels below the line are occupied and those above unoccupied. The localized level in the TLM model derived from equation (3.8) is shown by the thin curve. When E_d is positive, the positions of the localized level of the TLM and SSH models agree remarkably well. The reason for the agreement is that the dimerization amplitude $\bar{y}_n$ varies weakly around the impurity as shown in figure 2(*a*), and thus the assumption $\Delta(x) = \Delta_0$ is good enough in the TLM model. When E_d is negative, it would be energetically more favourable to generate two independent solitons than to keep the localized level, predicted by the TLM model, unoccupied. This would be the main reason for disagreement in the case $E_d < 0$. From the data of wavefunctions, we find that the level, whose energy is near zero, is associated with the free soliton, and the other gap level is of the pinned soliton. The mid-gap level of the free soliton is insensitive to E_d. Weak change would originate from mixing of levels due to the finite system size. Change of the energy level associated with the pinned soliton is explained well by the single-soliton solution of the TLM model. This will be discussed in section 4.

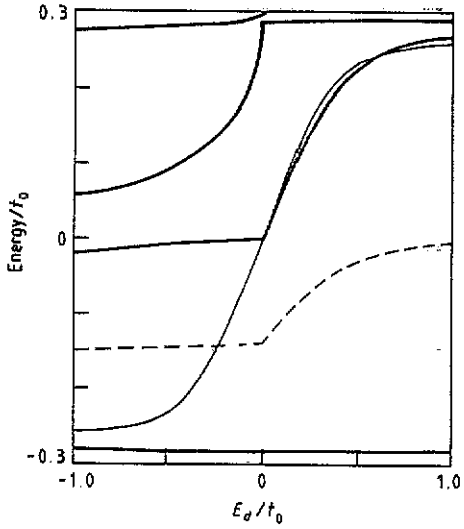

Figure 4. Electronic level structure around the Peierls gap as a function of E_d in the SSH model. Parameters are $V = 0.5t_0$ and $N = N_e = 50$. The Fermi level is denoted by the broken curve. The thin curve is the result by the TLM model, obtained in section 3.1.

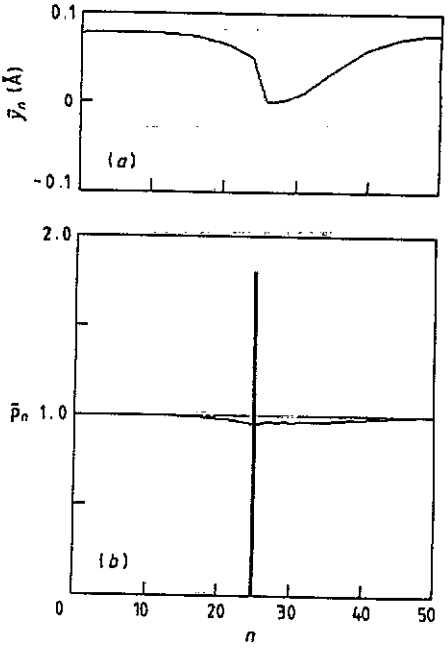

Figure 5. Dimerization pattern (a) and electron density (b) in the SSH model with an Anderson impurity at $n = 25$. In (b), electron number at the d level is also shown by the vertical bar. Parameters are $V = 0.5t_0$, $E_d = -0.6t_0$, $N = 50$ and $N_e = 51$.

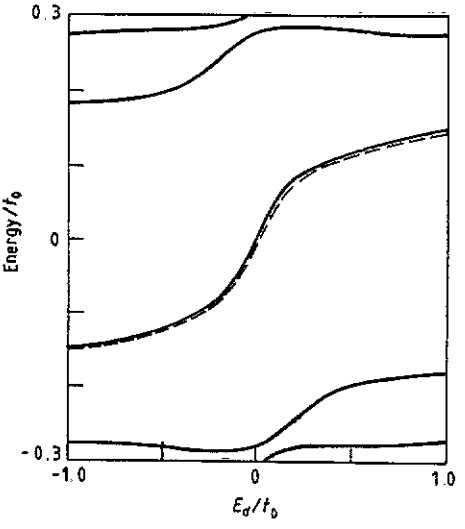

Figure 6. Electronic level structure around the Peierls gap as a function of E_d in the SSH model. Parameters are $V = 0.5t_0$, $N = 50$ and $N_e = 51$. The Fermi level is denoted by the broken curve. It is identical to one of the thick curves.

3.2.2. $N_e = N + 1$. This part is devoted to systems with $N_e = N + 1$. In other words, half-filled systems are considered. First, we present typical numerical solutions in figure 5. The d level is $E_d = -0.6t_0$. We find a trapped polaronic distortion around the impurity at $n = 25$ in figure 5(a). As shown in figure 5(b), the d level is nearly doubly filled. Then, the electron number of the chain is less than half-filled by about one. The lattice distortion, thus, is associated with a positive polaron trapped by an effective site-type impurity with strength $0.417t_0$. The distortion is asymmetric with respect to the impurity because of the alternation of strong and weak bonds. The tail of the distortion at $n > 25$ is longer than that at $n < 25$. This is correlated with the longer tail of the charge reduction at $n > 25$, found in figure 5(b).

Numerical solutions for positive E_d are similar to those for negative E_d. For example, lattice distortion for $E_d = 0.6t_0$ is the same as that in figure 5(a). Charge density for $E_d = 0.6t_0$ is obtained, by calculating $1 - \bar{\rho}_n$ from the data of figure 5(b). We obtain a trapped negative polaron in this case.

Energy levels around the Peierls gap are shown as a function of E_d in figure 6. The full curves are the results of the present calculation. The Fermi level is denoted by the broken curve, which is identical to the singly occupied level in the energy gap. Two localized levels associated with the polaron change their energies as E_d varies. The positive polaron gradually changes into the negative polaron with increasing E_d.

3.2.3. $N_e = N + 2$. Numerical results for this case can be obtained from those of section 3.2.1 by performing the charge conjugation transformation and replacing E_d with $(-E_d)$. Then, we can obtain a localized level at the top of the conduction band when $E_d < 0$. The level would be well explained by the TLM results in section 3.1. We would get a pinned soliton and a free soliton if $E_d > 0$.

To summarize section 3.2, we have shown that a new localized state appears in the energy gap when there is an Anderson impurity. This fact is supported by the remarkable agreement between solutions of TLM and SSH models when the dimerization is nearly perfect. On the other hand, our calculations also reveal the limitation of the uniform order parameter. We cannot treat cases where it is energetically favourable to create solitons or polarons. In these cases, the energy level structures are completely different from those of the nearly dimerized system. We find complex mixing between mid-gap levels associated with non-linear excitations and the localized state due to the impurity.

4. Systems with odd sites

When a chain is composed of an odd number of sites, there is a soliton in the impurity-free case. There is one localized level associated with the soliton at the gap centre. If this level is singly occupied, the soliton has no charge but spin. It is called a neutral (spin) soliton. When the level is filled or empty, the soliton has unit charge but no spin. It is named a charged soliton. In this section, we investigate how electronic structure changes when an Anderson impurity is present. The model is analysed as functions of localized level and electron number.

4.1. TLM model

It is well known that the TLM model (2.5) has a soliton solution centred at $x = 0$. The order parameter is

$$\Delta(x) = \Delta_0 \tanh(x/\xi) \tag{4.1}$$

where $\xi = v_F/\Delta_0$ is the coherence length. The wavefunctions and eigenvalues are

$$\psi_k(x) = \frac{e^{ikx}}{2L^{1/2}} \begin{pmatrix} 1 + [v_F k + i\Delta(x)]/\varepsilon_k \\ i\{1 - [v_F k + i\Delta(x)]/\varepsilon_k\} \end{pmatrix} \qquad \varepsilon_k = \pm[(v_F k)^2 + \Delta_0^2]^{1/2} \tag{4.2}$$

for the conduction and valence bands, and

$$\psi_b(x) = \frac{\operatorname{sech}(x/\xi)}{2\xi^{1/2}} \begin{pmatrix} 1 \\ -i \end{pmatrix} \qquad \varepsilon_b = 0 \tag{4.3}$$

for the mid-gap state. We calculate how energy level structure changes in the presence of the Anderson impurity at the lth site.

By making an equation of motion, we obtain the d-electron's Green function

$$G_d(i\varepsilon_n) = \left(i\varepsilon_n + \mu - E_d - aV^2 \sum_\kappa \mathrm{Tr}[\psi_\kappa(x_l) G_c^{(0)}(\kappa, i\varepsilon_n) \psi_\kappa^*(x_l)] \right)^{-1} \tag{4.4}$$

where the sum with respect to κ is taken over the valence and conduction bands, and the mid-gap state. Using (4.2) and (4.3) and $G_c^{(0)}(\kappa, i\varepsilon_n) = (i\varepsilon_n + \mu - \varepsilon_\kappa)^{-1}$ ($\kappa = k, b$), we obtain

$$\sum_\kappa \psi_\kappa(x_l) G_c^{(0)}(\kappa, i\varepsilon_n) \psi_\kappa^*(x_l) = -\frac{1}{2v_F[\Delta_0^2 - (i\varepsilon_n + \mu)^2]^{1/2}} \times \left[i\varepsilon_n + \mu + \Delta(x_l)\sigma_1 + \frac{\sigma_2 - 1}{2(i\varepsilon_n + \mu)} \Delta_0^2 \operatorname{sech}^2\left(\frac{x_l}{\xi}\right) \right]. \tag{4.5}$$

Inserting equation (4.5) into (4.4) gives

$$G_d(i\varepsilon_n) = \left\{ i\varepsilon_n + \mu - E_d + \frac{V^2}{2t_0} \frac{1}{[\Delta_0^2 - (i\varepsilon_n + \mu)^2]^{1/2}} \times \left[i\varepsilon_n + \mu - \frac{1}{2(i\varepsilon_n + \mu)} \Delta_0^2 \operatorname{sech}^2\left(\frac{x_l}{\xi}\right) \right] \right\}^{-1}. \tag{4.6}$$

When the limit $x_l \to \pm\infty$ is taken, we recover equation (3.7). The condition for the singularity of (4.6) is

$$(\Delta_0^2 - \omega^2)^{1/2} = \frac{V^2}{2t_0} \left(\frac{\omega}{E_d - \omega} - \frac{\Delta_0^2 \operatorname{sech}^2(x_l/\xi)}{2\omega(E_d - \omega)} \right) \tag{4.7}$$

where $i\varepsilon_n + \mu$ is replaced by ω. This equation has two solutions in the energy gap. One of them corresponds to the mid-gap state, and the other is the new localized state discussed in section 3.1. In the next subsection, the numerical solutions will be shown by thin curves in figures 8 and 10, and will be compared with SSH results.

We discuss the solution and relations to that of section 3. When $|E_d| \ll \Delta_0$, we can replace the left-hand side of (4.7) by Δ_0. The approximate solution is

$$\omega \simeq \frac{1}{2(\Delta_0 + V^2/2t_0)} \left\{ E_d\Delta_0 \pm \left[(E_d\Delta_0)^2 + \frac{V^2\Delta_0^2}{t_0} \operatorname{sech}^2\left(\frac{x_l}{\xi}\right) \left(\Delta_0 + \frac{V^2}{2t_0}\right) \right]^{1/2} \right\}. \tag{4.8}$$

If $|x_l| \to \infty$, we recover the solution (3.9) and the mid-gap level (4.3).

We consider an interesting limit $|E_d| \gg \Delta_0$. When $|\omega| \ll \Delta_0$ and $|E_d| \gg \Delta_0$, we retain only dominant terms in (4.7) to get

$$\Delta_0 \simeq -(V^2/2t_0)/\Delta_0^2 \operatorname{sech}^2(x_l/\xi)/2\omega E_d. \tag{4.9}$$

Then, the solution is

$$\omega \simeq -V^2\Delta_0 \operatorname{sech}^2(x_l/\xi)/4t_0E_d. \tag{4.10}$$

We find that the energy of the mid-gap state shifts due to the impurity.

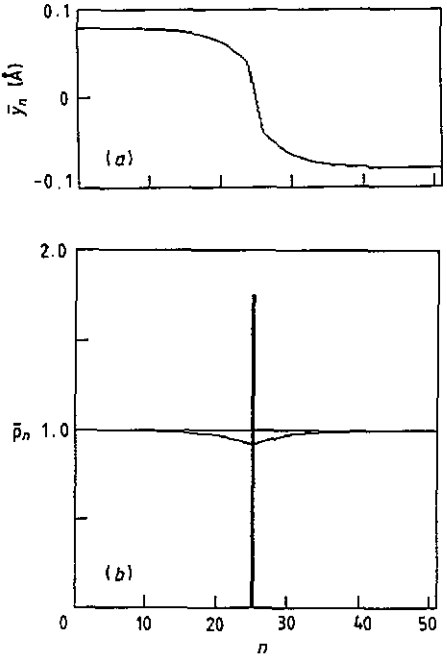

Figure 7. Dimerization pattern (*a*) and electron density (*b*) in the SSH model with an Anderson impurity at $n = 25$. In (*b*), electron number at the d level is also shown by the vertical bar. Parameters are $V = 0.5t_0$, $E_d = -0.6t_0$, $N = 51$ and $N_e = 52$.

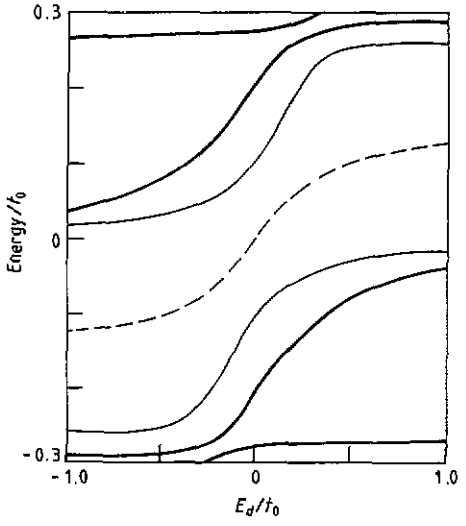

Figure 8. Electronic level structure around the Peierls gap as a function of E_d in the SSH model. Parameters are $V = 0.5t_0$, $N = 51$ and $N_e = 52$. The Fermi level is denoted by the broken curve. The thin curves are the results by the TLM model, obtained in section 4.1.

When $|\omega| \sim \Delta_0$ and $|E_d| \gg \Delta_0$, the dominant contribution in (4.7) yields

$$(\Delta_0^2 - \omega^2)^{1/2} \simeq \frac{V^2}{2t_0}\left(\frac{\omega}{E_d} - \frac{\Delta_0^2 \operatorname{sech}^2(x_l/\xi)}{2\omega E_d}\right). \tag{4.11}$$

The approximate solution is

$$\omega \simeq \Delta_0(\operatorname{sgn} E_d)\left[1 - \frac{1}{8}\left(\frac{V^2}{2t_0}\right)^2 \frac{[1 + \tanh^2(x_l/\xi)]^2}{E_d^2} + O\left(\left(\frac{V^2}{2t_0}\right)^3\right)\right]. \tag{4.12}$$

Thus, the localized level in the impurity equation (3.10) is also shifted by the soliton. Solutions (4.10) and (4.12) have shifted in opposite directions. If the energy shift of one of them is positive, that of the other is negative. This may be due to the level repulsion effect.

4.2. SSH model

The model equation (2.1) is to be studied numerically. In this subsection, we use $N = 51$. Other parameters are the same as those in section 3.2.

4.2.1. $N_e = N + 1$. There are $2(N + 1)$ electronic states in the whole system. Thus, electron number is at half-filling in this part of the subsection. Figure 7 shows lattice configuration and charge density distribution for $E_d = -0.6t_0$. We find a pinned soliton

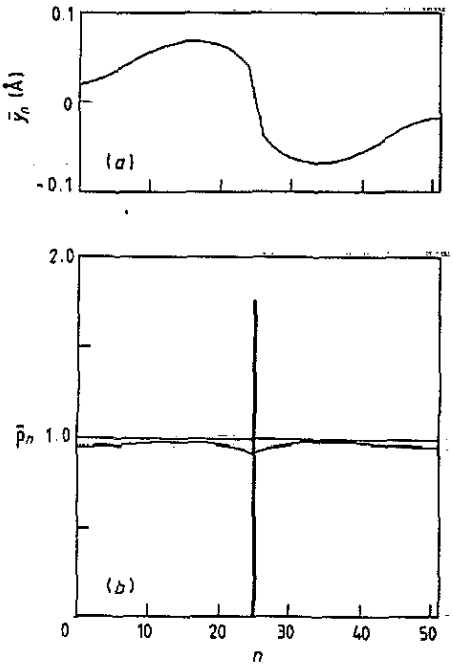

Figure 9. Dimerization pattern (a) and electron density (b) in the SSH model with an Anderson impurity at $n = 25$. In (b), electron number at the d level is also shown by the vertical bar. Parameters are $V = 0.5t_0$, $E_d = -0.6t_0$ and $N = N_e = 51$.

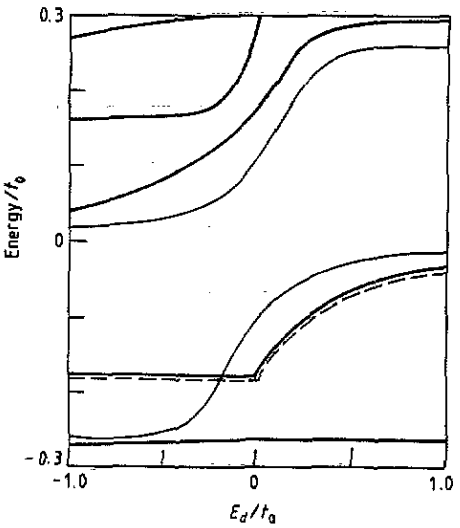

Figure 10. Electronic level structure around the Peierls gap as a function of E_d in the SSH model. Parameters are $V = 0.5t_0$ and $N = N_e = 51$. The Fermi level is denoted by the broken curve. It is identical to one of the thick curves. The thin curves are the results by the TLM model, obtained in section 4.1.

around the impurity at $N \simeq 25$. Change of $\bar{y}_n$ is steeper around the impurity. Filling of the d level is about two. Then, number of π electrons is about $N - 1$. This number is less than the value N at half-filling. So, the soliton is positively charged.

When E_d is positive and large enough, the d level is almost empty. The chain system has excess electron number, which is near to one. The soliton is negatively charged in this case. As E_d increases from negative to positive value, the positive soliton gradually changes into the negative one.

Change of energy levels around the Peierls gap is shown in figure 8. The broken curve indicates the Fermi level. It is defined by the average value of the highest occupied and the lowest unoccupied states. The thin curves are numerical solutions of equation (4.7). When $E_d < -\Delta_0$, the upper curve corresponds to the mid-gap level and the lower one to the bound state at the impurity. When E_d becomes larger, the two states mix with each other and are not discernible. Finally, when $E_d > \Delta_0$, the upper level becomes the impurity state and the lower level corresponds to the mid-gap level of the soliton. Overall variations of the two localized levels agree well with the TLM results. But, the agreement is not as good as that in section 3. This may be due to the fact that the local narrowing of the soliton width at the impurity is not taken into account in the previous subsection. The narrowing of the soliton implies decrease of the coherence length. So, the local energy gap becomes wider. The localized impurity state also moves apart from the gap centre. In this way, the absolute values of the energies of the two levels are larger in the SSH model than in the TLM model.

4.2.2. $N_e = N$. In this part, we look at solutions of the system with $N_e = N$. Electron number decreases from half-filling. In figure 9, we show $\bar{y}_n$ and $\bar{\rho}_n$ for $E_d = -0.6t_0$. The d level is almost full. Thus, the number of π electrons is nearly $N - 2$. In figure 7(a), the mid-gap state of the system is empty. An electron is removed from the top of the valence band of the system in figure 7 to obtain the system of figure 9. It will be energetically favourable to create an additional non-linear excitation. In this case, a new polaron is formed far from the impurity site. The charge distribution of π electrons reflects the presence of the pinned soliton and the almost free polaron.

When E_d is positive and large enough, the localized d level is almost empty. The number of π electrons is about N. Then, the mid-gap level shown in figure 8 accepts one electron. The positively charged soliton in section 3.2.1 changes into a nearly neutral soliton. Variation of $\bar{y}_n$ is almost the same as that in figure 7(a).

We depict energy levels around the Peierls gap in figure 10. The broken curve is the Fermi level, which is identical to the singly occupied level in the Peierls gap. The thin curves are the TLM results. When $E_d > 0$, overall agreement between SSH and TLM results is found. However, if $E_d > 0$, the level structure is different. The level, which varies similarly to the thin curve, is associated with the trapped soliton. The other two mid-gap levels are of the free polaron and they are almost independent of E_d. In this way, coexistence of mid-gap levels of the soliton and polaron is found.

4.2.3. $N_e = N + 2$. When $N_e = N + 2$, the system is the electron-doped one like that of section 4.2.1. Change of electronic structure is opposite to the change from section 4.2.1 to section 4.2.2. Numerical results can be obtained from those of the system with $N_e = N$, by performing charge conjugation transformation and replacing E_d with $(-E_d)$. Then, we would obtain a nearly neutral soliton when $E_d < 0$. We would get a free polaron and a pinned negative soliton if $E_d > 0$.

To conclude section 4.2, we have shown overall agreement on the electronic localized levels between SSH and TLM models when single-soliton solutions are stable. The remaining difference comes from the local variation of the order parameter around the impurity.

5. Summary and discussion

We have shown that a new localized state appears around the Anderson impurity in conjugated polymers. We have concentrated upon the systems with $U = 0$. Effects of finite U will be studied in the following paper [14].

First, the presence of the localized state is shown by analytic investigation of the TLM model. When the order parameter is uniform, a new state is located at the top of the valence band with negative impurity level. It is localized at the bottom of the conduction band if the impurity level is positive and in the conduction band. Furthermore, we have shown that the localized level is also present in the gap when there is a soliton. In this case, there are two localized levels in the gap. One is associated with the impurity and the other is the mid-gap state of the soliton.

Next, the SSH model with finite system size is diagonalized in order to establish the TLM results. We have shown the good agreement between the TLM and SSH results when the TLM order parameters are stable against the extra change of the electron number. In section 3.2, the localized level in the TLM model agrees remarkably well with that in the SSH model when the nearly dimerized system is the stable solution. In section 4.2, we find similar agreement when the single-soliton solution is stable. But, the agreement in

section 4.2 is not as good as in section 3.2, owing to the steep change of the order parameter around the impurity. On the other hand, we do not find any agreement when the extra change of electron number is important. In this case, there are complex mixed levels in the gap. They originate from the localized level around the impurity and the mid-gap states with respect to non-linear excitations.

In view of the above new findings, we should remark on relations to realistic defects in conjugated polymers. When the impurity is a dopant, the d level is embedded in the valence or conduction band. The localized level appears in the gap. The position is explained by whether the dopant is an acceptor or a donor. When it is an acceptor, the d level is filled up with electrons and the localized level is at the top of the valence band. If it is a donor, the d level is unoccupied and the new level is at the bottom of the conduction band. These discussions agree well with those of the site-type impurity effects previously investigated [3, 7]. The quantitative equivalence has been shown in section 3.1 and the appendix of the present paper. The energy of the localized level in the gap agrees well with that of the site-type impurity problem [7] with strength $J = -V^2/E_d$.

When the impurity is a carbonyl defect, the d level would be in the valence band as Mizes and Conwell noted [11]. The quantity E_d is the site energy of the π electrons of the oxygen and the mixing V indicates the π bond between the carbon and the oxygen. A new level appears at the top of the valence band. This level seems not to have been found in experiments. This may be due to the fact that resolution is not very good in photospectroscopic experiments. Better resolution is to be expected.

For an atomic side group, it seems that our model is too simple. However, we believe that fundamental effects on the polymer chain due to the defect are modelled by our simple Anderson impurity. We can expect that a new level would appear in the electronic gap in general. The detailed structures of the localized level would depend on electronic structures of the atomic side group and forms of interactions with the polymer chain.

We have considered only systems with no Coulomb interaction. Even if it is present, the new feature, the existence of the localized level, would not be changed. But, when the Coulomb strength at the d level is large enough, filling of electrons of this level changes. We will quantitatively discuss effects of Coulomb interaction in the next paper [14].

In [9], we have numerically investigated site-type impurity effects on soliton–lattice systems. We have not obtained any information on localized states in the gap because of the smallness of number of states around the gap. Judging from the results of the present paper, we expect similar localized levels around solitons trapped by impurities. Quantitative discussion will await future investigations.

We have only investigated the single-impurity problem. The many-impurity problem can be formulated with the help of the coherent potential approximation. This approximation has recently been used in the Anderson alloy system in order to discuss electronic properties of heavy fermion alloys [15]. Study of the system with many Anderson impurities (with random distribution) is also an interesting problem, which awaits future research.

Acknowledgments

Fruitful discussions with Professor Y Wada and Dr A Terai are acknowledged. Numerical investigations have been performed on HITAC M-680 and S-820 of the Computer Center of the University of Tokyo, and also on HITAC M-680 and S-820 of the Institute of Molecular Science, Okazaki National Research Institutes.

Appendix. Equivalence between the Anderson impurity (with $U = 0$) and the site-type impurity

In this appendix, we verify the equivalence between the Anderson impurity and the site-type impurity, discussed in association with the solutions (3.10) and (3.11). Hereafter, we assume the relation $|E_d| \gg V$.

The Anderson impurity (2.3) takes the form

$$H'_A = E_d \sum_s d_s^\dagger d_s + V \sum_s (d_s^\dagger c_{l,s} + c_{l,s}^\dagger d_s) \tag{A1}$$

at $U = 0$. We perform a unitary transformation in order to eliminate the mixing term as follows:

$$\tilde{H}_A = e^S H'_A e^{-S} \tag{A2}$$

where S is an anti-Hermitian operator. We can particularly take

$$S = g \sum_s (d_s^\dagger c_{l,s} - c_{l,s}^\dagger d_s) \tag{A3}$$

where g is assumed to be real and proportional to V. We expand (A2) up to second order in V:

$$\tilde{H}_A \simeq H_A^{(0)} + H_A^{(1)} + [S, H_A^{(0)}] + [S, H_A^{(1)}] + \tfrac{1}{2}[S, [S, H_A^{(0)}]] + O(V^3) \tag{A4}$$

where

$$H_A^{(0)} = E_d \sum_s d_s^\dagger d_s \tag{A5}$$

and

$$H_A^{(1)} = V \sum_s (d_s^\dagger c_{l,s} + c_{l,s}^\dagger d_s). \tag{A6}$$

The quantity g is to be determined by the condition

$$H_A^{(1)} + [S, H_A^{(0)}] = 0. \tag{A7}$$

This implies that the terms of first order in V cancel each other in (A4). Using equations (A3), (A5) and (A6), we get

$$g = V/E_d. \tag{A8}$$

Inserting equations (A5), (A6) and (A8) into (A4), we finally obtain

$$\tilde{H}_A = \left(E_d + \frac{V^2}{E_d}\right) \sum_s d_s^\dagger d_s - \frac{V^2}{E_d} \sum_s c_{l,s}^\dagger c_{l,s}. \tag{A9}$$

The second term of equation (A9) indicates that the model (A1) is equivalent to the site-type impurity $H_1 = J \Sigma_s c_{l,s}^\dagger c_{l,s}$ with $J = -V^2/E_d$, under the condition $|E_d| \gg V$. This is the evidence that solutions (3.10) and (3.11) agree in the limit $|E_d| \gg \Delta_0$ when a relation $J = -V^2/E_d$ is assumed.

References

[1] Harigaya K, Wada Y and Fesser K 1989 *Phys. Rev. Lett.* **63** 2401
[2] Harigaya K, Wada Y and Fesser K 1990 *Phys. Rev.* B **42** 1268

[3] Harigaya K, Wada Y and Fesser K 1990 *Phys. Rev.* B **42** 1276
[4] Harigaya K, Wada Y and Fesser K 1990 *Strongly Coupled Plasma Physics* ed S Ichimaru (Amsterdam: Elsevier; Tokyo: Yamada Science Foundation) p 255
[5] Harigaya K 1990 *J. Phys. Soc. Japan* **59** 1348
[6] Harigaya K, Wada Y and Fesser K 1990 *Phys. Rev. Lett.* **65** 806
[7] Harigaya K, Wada Y and Fesser K 1990 *Phys. Rev.* B **42** 11303
[8] Harigaya K, Terai A, Wada Y and Fesser K 1991 *Phys. Rev.* B **43** 4141
[9] Harigaya K and Terai A 1991 *Solid State Commun.* **78** 335; *Phys. Rev.* B preprint
[10] Anderson P W 1961 *Phys. Rev.* **124** 41
[11] Mizes H A and Conwell E M 1991 *Proc. Int. Conf. on Science and Technology of Synthetic Metals 1990* unpublished
[12] Takayama H, Lin-Liu Y R and Maki K 1980 *Phys. Rev.* B **21** 2388
[13] Su W-P, Schrieffer J R and Heeger A J 1980 *Phys. Rev.* B **22** 2099
[14] Harigaya K 1991 *J. Phys.: Condens. Matter* **3** 4857
[15] Harigaya K 1990 *J. Phys.: Condens. Matter* **2** 4623